ELSEVIER

Journal of Nuclear Materials 258–263 (1998) 345–350

journal of nuclear materials

Comparative analysis of copper alloys for the heat sink of plasma facing components in ITER

G. Kalinin *, R. Matera

ITER Garching JWS, Max-Planck-Institute fur Plasmaphysik, Boltzmannstrasse 2, D-85748 Garching bei Munchen, Germany

Abstract

Due to their excellent thermal conductivity, copper alloys are the obvious choice for the heat sink of the high heat flux (HHF) components in ITER. In addition to thermal conductivity, other properties have to be taken into consideration for the final selection of the alloy system and of the specific grade. For comparison, the following parameters have been taken into account: tensile strength and ductility, fracture toughness, allowable strain for fatigue endurance of 10^4 cycles, thermal stress factor, and thermal conductivity. An assessment is made of the proposed copper alloys to be used in ITER, precipitation hardened copper alloys (CuCrZr, CuNiBe, CuNiCrSi) and dispersion hardened copper (CuAl25). The analysis shows that CuAl25 is the most reasonable choice for the HHF components of the primary wall due to heat resistance and satisfactory design allowable (strength, fatigue and fracture toughness), CuCrZr is proposed for the divertor where the fatigue and resistance to fracture are most critical.

1. Introduction

In the design of ITER Plasma Facing Components (PFCs), a high thermal conductivity material, the heat sink, is interposed between the armour and the cooling circuit. The main function of the heat sink is to transport elevated heat fluxes to the cooling water, thus reducing thermal stresses in the structural material, namely an austenitic stainless steel, to acceptable levels. Two families of copper alloys exhibit high thermal conductivity, strength and radiation resistance, precipitation hardened (PH) and oxide dispersion strengthened (DS) alloys. Within each class, different alloys are commercially available, CuCr, CuCrZr, CuNiBe, CuNiCrSi, among the PH alloys; GlidCop Al15, Al25, Al60 and MAGT-0.2 among the DS alloys. Comparative analyses of copper alloys were performed by several authors [1–4]. Additional data were obtained during the ITER R&D activity. The aim of this paper is to compare the properties of the candidate alloys, in the unirradiated condition.

The analysis includes four alloys CuCrZr-IG, CuNiBe, CuCrNiSi and CuAl25-IG. The CuCrZr-IG and CuAl25-IG represent the commercial alloys which have been optimised for the ITER application and designated as IG-ITER Grade.

2. Working conditions

Copper alloys are used in the form of either tubes or plates with passages for the cooling channel; in the primary wall and baffle, a stainless steel liner is located in the copper plates. In the components subjected to the highest heat fluxes (divertor and limiter), the copper heat sink structure is directly cooled by water. The design of the ITER high heat flux components are described in [5,6]. Table 1 gives the design working conditions of copper alloys for the different HHF components.

3. Design criteria and properties used for comparative analysis

The structural design criteria used for the design and lifetime evaluation of the ITER in-vessel components

* Corresponding author. Tel.: +49 89 3299 4123; fax: +49 89 3299 4163; e-mail: kalinig@sat.ipp-garching.mpg.de.

0022-3115/98/$19.00
PII: S0022-3115(98)00271-2

Table 1
In-vessel components containing copper alloys: Design parameters for the BPP of ITER

Component	Dose of irrad. (dpa)	Temperature (°C)	Working condition	Pulse parameters		
				Av/peak heat load, MW/m2	No. of pulses max.	Max. time, (s)
PW	3.0	140–245	Normal pulse	0.25/0.5	10 000	1000
Limiter	3.0	140–172	Normal pulse	0.25/0.5	15 000	1000
		140–398	Start-up and shut-down	3.8/8	10 000 × 2	50–100
Baffle	3.0	140–246	Normal pulse	1/3	10 000	1000
Dome, upper VT	0.4–0.5	150–300	Normal pulse	5/5	3000	1000
Dump target, lower VT	0.1–0.4	150–280	Normal pulse	5/20	3000	1000
Cassette liner	0.03–0.06	150–300	Normal pulse	0.3/0.7	3000	1000

Note: The number of pulses for the divertor are given for the PFC's assuming three replacement times during BPP.
The off-normal events (disruptions, VDE, accident, etc.) are not included in the table.
All components are subjected to baking at 240°C with duration ~120 h, up to 100 times.
PW – primary wall, VT – vertical target.

are described in [7]. In the initial stage of the design, only the stress limits were taken into consideration for the principal design solution. The detailed analysis should include both elastic analysis and inelastic analysis.

For the comparative analysis of different candidate materials the tensile properties, ultimate strength, S_u, yield strength, S_y and uniform elongation, fracture toughness K_{1c} (or J_{1c}) and the fatigue strain at 10^4 cycles were taken into account. Thermal conductivity, k_{th}, and thermal expansion, α, were also included in the assessment of the materials applicability for the high heat flux components. The capability of material to withstand thermal loads is expressed by the factor $M = S_m k_{th}(1 - \nu)/\alpha E$, where ν is Poisson's ratio, E is Young's Modulus and S_m is stress intensity limit. These selected properties are used to characterise the general materials behaviour in the HHF components.

4. Properties of candidate copper alloys

The composition, heat treatment and properties of CuCrZr-IG alloy are presented in [8,9]. The heat treatment of CuCrZr-IG is: solution anneal (SA) at 980–1000°C for 1 h, water quench, then age at 450–480°C for 2–3 h. The optimal heat treatment usually includes intermediate cold work after SA that gives better strength. CuAl25-IG is the modified Glidcop Al25 DS alloy produced by OMG Americas. Its properties are given in [7–9]. Data on CuNiCrSi were published in [1,10]. Heat treatment: SA at 950–100°C for 1 h, cold work 40–70% and age at 470°C for 4 h. CuNiBe data were presented in several papers [2,4,11–16]. Data of Hycon 3 HP (temper: TM04 ASTM B 601) produced by Brush Wellman Inc. were used as a Ref. [11].

The available data on the properties of given material are too scattered to allow proper comparison. The data were first analysed for each material and an averaged data base was generated. The comparison is based on the average data. The properties of copper alloys were analysed in a wider temperature range (20–500°C), than that of the working conditions of copper alloys in the HHF components during normal operation cycles.

The analysis of physical properties shows that the difference in the density of all four alloys is negligible, ~1%. A larger variation is found in the thermal expansion coefficient, but these variations are no more than ~8%. The most significant difference is in the Young's Modulus and in the thermal conductivity. Thermal conductivity is highest for CuCrZr-IG alloy and lowest for CuNiCrSi (see Fig. 1). Above 300°C, the difference reduces, and both CuNiBe and CuAl25-IG have almost the same thermal conductivity. The thermal conductivity affects the temperature gradient in the wall of HHF components and hence the thermal stresses, but this

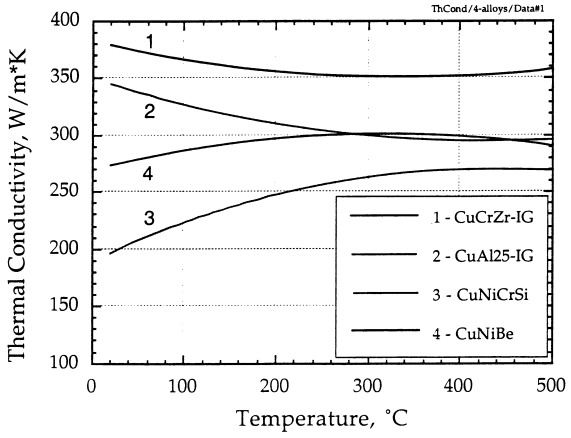

Fig. 1. Thermal conductivity of copper alloys.

difference is within 15–20%, and this variation is not critical for the design. Nevertheless, high thermal conductivity is preferable for the HHF components.

Tensile properties of copper alloys are shown in Fig. 2. CuNiBe exhibits a better thermal stress factor M than the other alloys. The strength of CuNiBe is almost a factor of two, higher than that of CuCrZr-IG and CuAl25-IG. The total elongation of CuCrZr-IG and CuAl25-IG is >24%, higher than that of CuNiCrSi and CuNiBe in the temperature range 20–500°C. The ductility of CuAl25-IG increases with increasing temperature, while that of CuCrZr remains relatively constant up to ~500°C. The total elongation of the other two alloys decreases with increasing temperature, going almost to zero above 400°C for CuNiBe. The ductility of CuNiBe at the temperatures exceeding ~400°C falls below the conventional ductility limit of 2% specified in the ITER Interim Structural Design Criteria (ISDC) [7]. This may have an impact on the materials behaviour during off-normal events or accidents. As shown in Fig. 2, total and uniform elongation practically coincide above 400°C. The loss of work hardening capability is related to a change in the fracture mode of CuNiBe, from ductile transgranular at room temperature and to ductile intergranular at elevated temperatures [17]. However the exact mechanism of such behaviour remains uncertain.

The uniform elongation of CuCrZr-IG slightly decreases above 300°C. No data are available for CuNiCrSi. Above 300°C [17] creep gives a significant contribution to the deformation of CuAl25-IG. A possible explanation of these observations is related to the microstructure of CuAl25-IG. The material is not completely homogeneous, as observed by transmission electron microscopy [18]. Alumina denuded regions of practically pure, soft copper, have been observed, which could be responsible for enhanced creep deformation in CuAl25-IG. Thermal creep should be taken into account for the HHF components design. Unfortunately, there is little information on creep of copper alloys in the relevant temperature range. This issue is being addressed in the planned R&D.

The allowable stress intensity limit, S_m can be estimated as min ($\frac{1}{3} S_{u,min}$; $\frac{2}{3} S_{y,min}$) [7]. For copper and it's alloys, S_m is dominated by the ultimate strength, not by the yield strength as it is for austenitic SS.

A systematic investigation of fatigue properties of CuAl25-IG, CuCrZr and CuNiBe was presented in [16,19,20]. The CuCrZr alloy used for the fatigue studies was solution annealed, cold worked and aged. Data on fatigue of CuNiCrSi are not available, but are likely to be similar to that of CuNiBe. Fig. 3 shows the strain amplitude ($\Delta\varepsilon$) dependence vs. the test temperature at

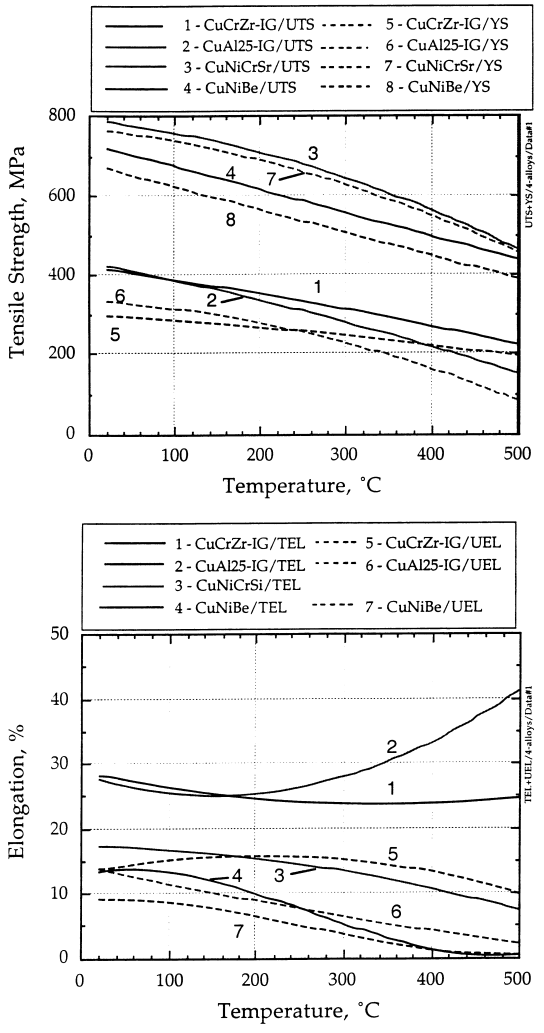

Fig. 2. Tensile properties of copper alloys; ultimate tensile strength – UTS, yield strength – YS, total elongation – TEL and uniform elongation – UEL.

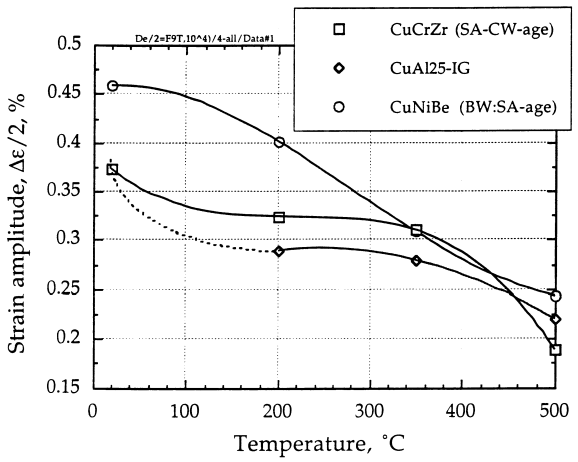

Fig. 3. Strain amplitude at 10^4 cycles of copper alloys.

10^4 cycles. Similar dependence is observed at 10^5 cycles. Below ~300–350°C, the strain amplitude at 10^4 cycles for CuNiBe is 20–30% higher than that of the other alloys. At temperatures >300–350°C low cycle fatigue life is the same for all alloys, but at these temperatures creep and the difference in deformation behaviour of these alloys may have a significant impact on the results. During normal operation conditions, the HHF components highest temperature of copper alloys is ~300°C. The fatigue life time of all alloys is very close at this temperature, while CuNiBe alloy shows better fatigue resistance at low temperature.

The available fracture toughness data (J_Q as a function of temperature) are shown in Fig. 4 [10,21–25]. For all alloys, fracture toughness decreases with increasing temperature. There is some scatter in the fracture toughness measurements performed by different laboratories. Most probably this difference is due to the material being processed in different ways and to the different testing methods. From a quantitative point of view, however, there is a striking difference between the fracture toughness of CuCrZr, which is higher in all temperature ranges, with respect to all other alloys. The precipitation hardened alloys (CuNiCrSi and CuNiBe) and CuAl25-IG exhibit much lower fracture toughness than CuCrZr. The testing environment has also an influence on the fracture toughness and on tensile properties [25].

To understand the importance of fracture toughness for the HHF components it is possible to estimate allowable crack size from the following equation:

$$[a] = \beta^2 \left(\frac{EJ_{1c}}{\sigma} \right)^2 \frac{(1 - a/h)^3}{3.275},$$

where β is the safety factor equal to either 0.33 or 0.67 depending on the criteria level, a/h is a ratio of crack depth to the thickness of section (0.25 ratio was assumed for this calculations), E is Young's Modulus, and σ is the maximum tensile stress oriented perpendicular to the crack. The primary membrane stress should be taken into account for the fast fracture criteria, and all types of local stress for the local fast fracture criteria (primary and secondary loading, including peak) [7].

The results of the calculation are presented in Fig. 5. Fig. 5 shows the dependence of the allowable crack depth vs tensile stress for two β values, 0.33 and 0.67. The results of the assessment show that HHF components made of CuCrZr-IG have a large margin against fast fracture within the allowable stress. CuAl25-IG and CuNiBe have very low values of the critical crack. Actually, the high strength and the high value of thermal stress factor of CuNiBe cannot be exploited, because the stress limit is defined by the fast fracture criteria. Both CuNiBe and CuAl25-IG have low allowable tensile stress (to prevent fast fracture). This calculation is not valid for the thin wall tubes (~1 mm). Nevertheless, similar quantitative comparison also can be extended to the cooling pipes.

5. Assessment of irradiation effect

On the basis of available data [2], it is estimated that electrical conductivity decreases 5–6% due to irradiation during the BPP of ITER. Taking into account the Wiedermann–Franz ratio, the same variation is expected for thermal conductivity.

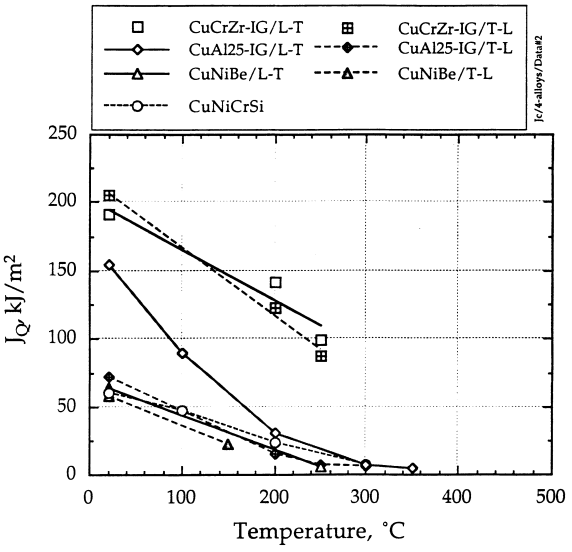

Fig. 4. Fracture toughness of copper alloys.

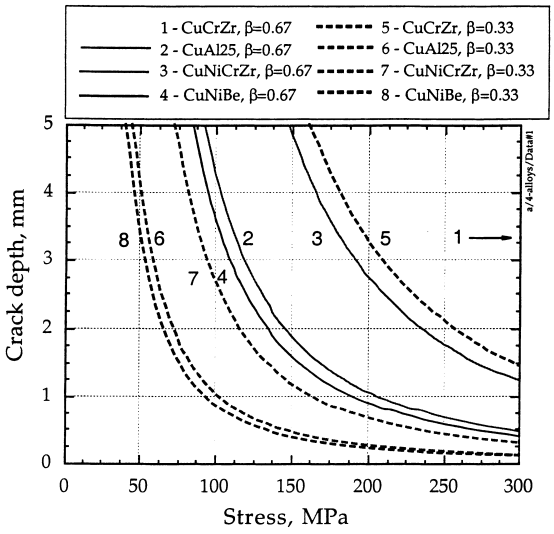

Fig. 5. Critical crack size of different copper alloys.

Neutron irradiation effects on mechanical properties of copper alloys depend strongly on temperature. At temperatures extending from room temperature to 250–300°C, radiation hardening is the dominant effect. Associated with radiation hardening, loss of work hardening capability and embrittlement occur. For the CuCrZr and CuAl25, radiation hardening disappear and radiation softening starts to produce its effects at temperatures exceeding the transition range, ~250–300°C. CuNiBe and CuNiCrSi exhibit brittle fracture after irradiation at ~250–300°C [2,26]. The fracture is transgranular, and the total elongation and the uniform elongation are the same, and in some cases decreases to zero. The strength of irradiated materials either decrease (for CuNiBe) or remain approximately at the same level as the unirradiated ones. The use of such a material with almost zero hardening capability and brittle intergranular fracture is not suitable for the HHF components where tensile stress concentration will occur.

DS Cu alloys show a decrease of uniform elongation (up to ~0.2–0.3%) after irradiation at 150°C and an increase after irradiation at 300°C. At the same time strength values remain no lower than that for unirradiated material. For design purposes the strength of unirradiated material is a conservative assumption for the stress analysis. The material fracture mode remains ductile at both temperatures. CuCrZr-IG has good uniform elongation in the unirradiated state. The uniform elongation decreases after irradiation at 150°C and 300°C but remains higher than 0.5% at 150°C and ~5% at 300°C.

There are no data on the fracture toughness of irradiated DS and PH copper alloys with the exception of one experiment on Glidcop Al15. Extremely low fracture toughness ($J_c \sim 1$ kJ/m^2) is measured after irradiation at 250°C for a dose ~2.5 dpa. Taking into account the fracture behaviour of copper alloys it is possible to predict that irradiated CuCrZr will have better fracture toughness in the temperature range (150–300°C) than the other alloys.

6. Conclusions

Both CuAl25-IG and CuNiBe can be used at tensile stresses below 100 MPa. The calculated tensile stress is about 23 MPa for the primary wall for the steady-state conditions. Such a stress will not result in fast fracture, and both materials could be used for the primary wall. CuAl25-IG was selected as the first option for the primary wall because (a) the stresses are within the design allowable including fracture criteria, and (b) it has better thermal stability under the manufacturing heat treatment. PH alloys will significantly change their properties after manufacturing (see Ref. [9]) which results in a decrease of allowable stress of CuCrZr, and to a lesser extent of CuNiBe and CuNiCrSi. If the manufacturing technology can be improved so that there is not a significant decrease in CuCrZr strength, this material should have priority.

For the divertor HHF components, local stresses are very high due to high heat flux and existence of singularity zones. The primary membrane and primary bending stresses are not critical for divertor HHF components, and are within the design allowable. More critical are local stresses that may result either in fatigue life or fracture limitation, in particular for the 20 MW/m^2 transients considered for the design. The material with better fracture resistance and fatigue endurance is preferred for these components. Fatigue lifetime is almost the same for all copper alloys analysed in the range 300–350°C. CuCrZr-IG, which has much better fracture toughness, is the preferred option for the divertor.

In the temperature interval 150–300°C, corresponding to the working temperature of PFCs, after neutron irradiation, CuCrZr-IG exhibits a better ductility and hardening capability than other alloys.

Acknowledgements

This paper was prepared as an account of work undertaken within the framework of the ITER EDA Agreement. The views and opinions expressed herein do not necessarily reflect those of the Parties to the ITER Agreement, the IAEA or any agency thereof. Dissemination of the information in this paper is governed by the applicable terms of the ITER EDA Agreement.

References

[1] G. Kalinin et al., Assessment and Characterisation of Candidate Cu Based Materials for the First Wall Application, RF HT RDIPE report ITER 4.2.42 (Moscow, 1994).
[2] S.J. Zinkle, S.A. Fabrisiev, in Fusion Materials, Semiannual Progress Report for Period Ending March 31, 1994, DOE/ER-0313/16, (US DOE, 1994), p. 314.
[3] G.J. Butterworth, C.B.A. Forty, J. Nucl. Mater. 189 (1992) 237.
[4] B. Singh, Assessment of Physical, Mechanical and Technological Properties of First Candidate Copper Alloys. Risø National Laboratory report R-769 (EN) (1994).
[5] R. Aymar, these Proceedings.
[6] K. Ioki et al., these Proceedings.
[7] ITER Interim Structural Design Criteria, ISDC, ITER report S 74 RE 2 97-07-30 W1.2 (1997).
[8] ITER Material Properties Handbook, MPH, ITER report S 74 MA2 98-04-14 W0.3 (1997).
[9] Materials Assessment Report, ITER report G A1 DDD 01 97-08-13 W0.1 (1997).
[10] A. Ivanov et al., J. Nucl. Mater. 233–237 (1996) 553.

[11] Guide to Beryllium Copper, Brush Wellman Inc. (1993).
[12] S. Zinkle and W. Eatherly, in: Fusion Materials, Semiannual Progress Report for Period Ending June 30, 1996, DOE/ER-0313/20 (US DOE, 1996) p. 207.
[13] J. Ratka and W. Spiegelberg, IEEE Trans. Magn. 30 (1994) 1859.
[14] J. Harkness et al., in: Metal Handbook, Vol. 2, American Society for Materials, Metals Park, OH, 1993, p. 403.
[15] K. Slattery, Copper Alloy Design Allowable, Private communication, 1997.
[16] K. Leedy, PhD Thesis, University of Illinois at Urbana–Champaign, IL 1997.
[17] S.J. Zinkle, W.S. Eatherly, in: Fusion Materials, Semiannual Progress Report for Period Ending December 31, 1996, DOE/ER-0313/21 (1997) p. 165.
[18] B. Singh, Private communication, 1997.
[19] J.F. Stubbins, Copper Alloy Performance: Fatigue. Report at the Working Meeting on Materials and Joints for In-vessel Components, G 73 RE 2 97-11-13 F1 (ITER, Garching JWS, 1996).
[20] K. Leedy et al., J. Nucl. Mater. 233–237 (1996) 547.
[21] R. Solomon, J. Troxell, A. Nadkarni. J. Nucl. Mater. 233–237 (1996) 542.
[22] D.J. Alexander, S.J. Zinkle, A.F. Rowcliffe, in: Fusion Materials, Semiannual Progress Report for Period Ending December 31, 1996, DOE/ER-0313/21 (US DOE, 1997) p. 175.
[23] S. Tahtinen, Explosion Welding of CuCrZr and 316LN IG. Report EURATOM-TEKES Association at the Working Meeting on Tasks T212&T213, G 73 RE 12 98-05-26 F 1 (ITER, Garching JWS, 1997).
[24] V. Prokhorov et al., Toughness of copper alloys MAGT-0.2, Paper 14001-P at the ICFRM-7, Obninsk, Russia, Sept. 1995.
[25] J. Alexander, B.G. Gieseke, in: Fusion Materials, Semiannual Progress Report for Period Ending December 31, 1996, DOE/ER-0313/21, 1997, p. 189.
[26] A. Ivanov et al., presented at the 8th Int. Conf. on Fusion Reactor Materials, Sendai, Oct. 1997.